

# Single-shot radiography using X-rays from Compton-backscattering with laser-wakefield accelerated electron beams

A. Döpp<sup>1,2</sup>, E. Guillaume<sup>1</sup>, C. Thaury<sup>1</sup>, J. Gautier<sup>1</sup>, I. Andriyash<sup>1</sup>, A. Lifschitz<sup>1</sup>, J-P. Goddet<sup>1</sup>, A. Tafzi<sup>1</sup>, V. Malka<sup>1</sup>, A. Rousse<sup>1</sup> and K. Ta Phuoc<sup>1</sup>  
<sup>1</sup> LOA, ENSTA ParisTech - CNRS - Ecole Polytechnique - Universit Paris-Saclay,  
828 bd des Marchaux, 91762 Palaiseau Cedex France and

<sup>2</sup> Centro de Laseres Pulsados, Parque Científico, 37185 Villamayor, Salamanca, Spain

We present results from the production of high energy femtosecond X-rays by Compton-backscattering of an intense femtosecond laser pulse with quasi-monoenergetic laser-accelerated electron beams using a plasma mirror. In our parameter regime electrons of  $\sim 150$  MeV peak energy emit a high energy radiation beam with a broad spectrum extending up to  $\sim 500$  keV. The photon yield from the source is sufficiently high to illuminate a centimeter-size sample placed 90 centimeters behind the source and record a single-shot radiograph. The small diameter of the laser-accelerated electron beams translates into a micrometer X-ray source size, making it a promising candidate for advanced X-ray imaging techniques as e.g. propagation-based phase contrast imaging.

X-rays illumination is one of the most important diagnostic used in medical imaging and industrial non-destructive testing. Conventional sources are primarily based on two processes that convert electron energy to high energy photon radiation: bremsstrahlung and synchrotron radiation [1]. Synchrotron sources can provide collimated, polarized, low bandwidth radiation [2], yet X-ray tubes using the simpler bremsstrahlung scheme are by far more common as source of X-rays. This is due to the size and costs of synchrotron lightsources, which typically consist of a GeV-level electron accelerator, a large scale storage ring and beam lines with insertion devices to produce radiation.

Laser-based light-sources have the potential to produce synchrotron type radiation in drastically reduced physical size and for a reasonable cost. Indeed, modern laser-plasma accelerators (LPAs) [3–6] allow acceleration of electron beams up to GeV energies over centimeter scale [7]. In addition to their compactness, such sources have a competitive normalized transverse emittance [8], due to their micrometer source size, and provide inherently ultrashort, femtosecond duration beams [9]. Furthermore, using an optical undulator instead of conventional magnetic structures allows to reduce the undulator period  $\lambda_0$  by 3-4 orders of magnitude. Therefore the combination of LPA with optical undulators allows to reproduce the principle of a synchrotron on a millimeter scale.

The radiation produced by scattering an intense laser by laser plasma accelerated electrons is very similar to conventional synchrotron radiation. As a main difference the peak deflection angle for scattering with an electromagnetic wave is given by  $a_0/\gamma$ , where  $a_0 \simeq 0.85\lambda[\mu\text{m}]\sqrt{I[10^{18}\text{W}/\text{cm}^2]}$  is the normalized vector po-

The experiment was performed with the Salle Jaune Ti:Sa Laser System at Laboratoire d'Optique Appliquée, which delivers linearly polarized laser pulses with 30

tential. We can express the the fundamental wavelength of backscattered photons as [10]

$$\lambda = \frac{\lambda_0}{2\gamma^2(1 - \beta \cos \phi)} \left( 1 + \frac{a_0^2}{2} + \gamma^2 \theta^2 \right).$$

In this optical expression,  $\phi$  is the angle between the laser beam and the electrons beam,  $\theta$  denotes the observation angle, while  $\beta = v/c_0$  and  $\gamma = (1 - \beta^2)^{-1/2}$  are the normalized electron velocity and the lorentz factor, respectively. Compton scattering can therefore lead to a frequency upshift of up to  $4\gamma^2$  of the incident radiation ( $hc_0/\lambda_0 \approx 1.55$  eV for a typical Ti:Sa laser wavelength of 800 nm).

The combination of LPA and backscattering is an experimentally challenging task, requiring extensive control of two terawatt-class laser pulses to overlap in time and space the electron beam and the scattering laser pulse, see for example [11, 12]. This is why this study uses a simpler all-optical method, based on the retro-reflection of a single laser pulse [13]. In this scheme, the intense drive pulse of the LPA is used for Compton scattering with the electrons traveling in its wake. To achieve this, the beam is back reflected by a plasma mirror, placed close to the exit of the LPA. The advantage of this scheme is that it ensures an inherent overlap of the electron beam and the laser pulse. In addition, it operates at 180 degree which permits the best conversion efficiency to high energy photons. While the first proof-of-principle experiment [13] showed a very broad photon energy distribution, recent studies have observed that scattering with quasi-monoenergetic electron beams can produce X-rays with about 50 percent energy spread at full width at half maximum (FWHM) [14]. Here we show that the X-ray signal of such backscattered beams is sufficient to radiography macroscopic samples.

femtosecond duration at full width at half maximum (FWHM). Using a spherical mirror of 700 mm focal length the  $\sim 1.6$  J pulse were focussed at the entrance of

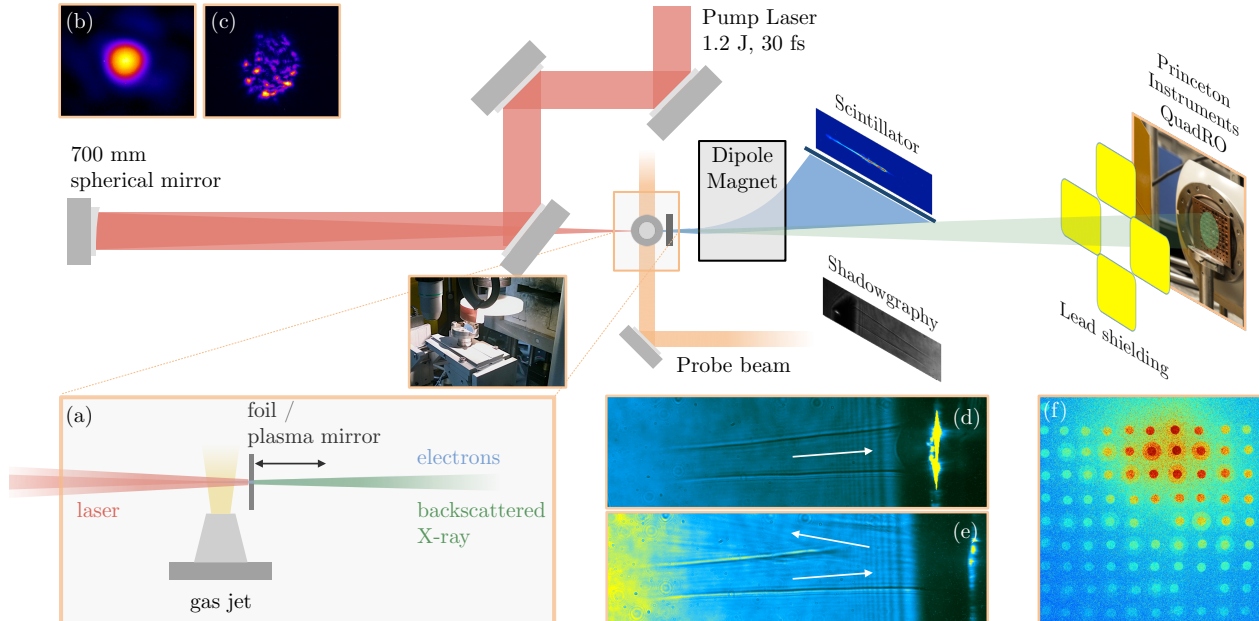


FIG. 1. Setup of the Compton backscattering experiment. The foil which acts as plasma mirror is placed at the exit of the gas jet, as shown in (a). The foil can be moved along the axis to distinguish between bremsstrahlung and backscattering. (b) shows the focal spot at the gas jet entrance. There are two diagnostics for the back-reflection: (c) shows an image of the backscattered light on the foil, which is recollimated using a lens system. Though not absolutely calibrated, this measures the relative intensity of the backscattered light. Also, when there is no reflection we observe a clear plasma channel on the shadowgraphy (d). Once the foil is in place we can also see the channel created from the reflected beam (e). The emitted X-rays are detected downstream on a Gadox scintillator, fiber-coupled to a low noise CCD (Princeton Instruments QuadRO). The temperature of the radiation is estimated using a filter array, as shown in (f).

a supersonic helium gas jet of 2 mm diameter, see Fig.2. The focal spot contained 50-55% of the beam energy.

The laser-plasma accelerator was operated in the transverse self-injection regime, producing beams of 300 - 600 pC charge at beam energies mostly in the range of 100 - 150 MeV. Electron charge and spectra were measured using a dipole magnet spectrometer combined with an absolutely calibrated phosphor screen. In contrast to previous experiments [13] the electron beams in this study had higher charge and showed important quasi-monoenergetic features, see Fig.2.

For the plasma mirror a 100  $\mu\text{m}$  cellophane foil was used. This choice of the plasma mirror material aims to reduce the production of bremsstrahlung as electrons pass through the plasma mirror. The foil is slightly inclined with respect to the laser axis in order to avoid back-reflection into the laser chain. It also permitted to observe the plasma channel created by the reflected beam in the gas jet, see. Fig.1e. Furthermore the reflected laser beam was imaged on a screen. After each shot the foil was translated to provide an undamaged mirror surface.

X-ray were detected using a GdOS based scintillator, fiber-coupled to a 16-bit CCD (Princeton Instruments

Quad-RO 4320). The total detector area was about  $5 \times 5 \text{ cm}^2$ , divided into  $2084 \times 2084$  pixels of 24  $\mu\text{m}$  edge length each. Placed on the laser axis at 90 centimeters from the interaction, this lead to a field of view of  $\sim 55 \times 55 \text{ mrad}^2$ .

Efficiency of the production of Compton scattering radiation depends on the intensity of the back reflected laser at the position of collision with the electrons. It therefore depends on the position of the foil with respect to the gas jet exit. As the Rayleigh length of the laser is about 0.8 millimeters, any signal observed for the foil placed at one centimeter behind the gas jet is not due to Compton backscattering but a result of bremsstrahlung produced by electrons passing through the foil. This background signal is rather stable, with a relative rms error of  $\sigma_{brems} \approx 0.1$ . When moving the foil inwards we observe a signal increase, up to about  $3.2 \pm 0.6$  times the bremsstrahlung background at the optimal foil position at the gas jet exit. These results are in agreement with previous studies [13].

Additionally, we could distinguish the signals due to their very different spectra. For this, we placed a 5.1 mm copper filter in front of the detector, which cuts off the spectrum below  $\sim 100 \text{ keV}$ . Holes inside the plate per-

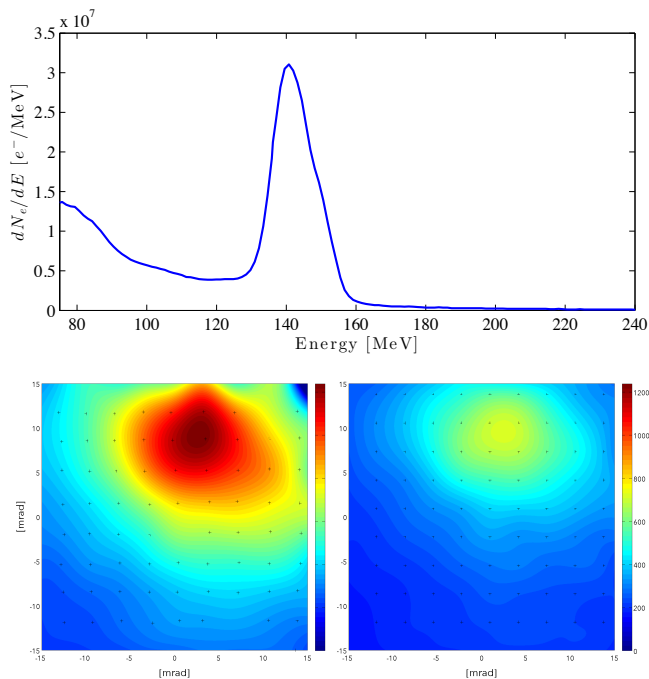


FIG. 2. Above: Typical electron beam spectrum used in the experiment. The spectrometer cuts electrons with energies below 75 MeV. Lower frame: Reconstructed signal of Compton backscattered radiation without (left) and with 5.1mm copper filter (right).

mit reconstruction of the unperturbed signal level, which is shown in Fig.2. The ratio between both the filtered signal  $I_1$  and the signal that passes through the holes  $I_0$  allows to roughly estimate the spectral content. We observe an important difference between the beams from Bremsstrahlung radiation and Compton backscattering. Shots with the foil close to the jet show a high contrast ratio of 0.6, the contrast being defined as  $1 - I_1/I_0$ . When

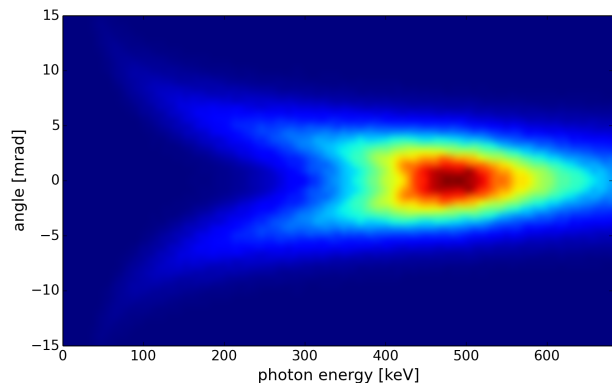


FIG. 3. Simulated angularly resolved spectrum of backscattered photons from the interaction of a laser-accelerated electron beam (140 MeV, 5 % energy spread, 5 mrad divergence) with a high power laser pulse ( $a_0 = 1.0$ , 30 fs).

moving the foil outwards the jet the contrast reduces to 0.1. This implies that the Compton X-ray are much more attenuated and therefore contain less signal beyond 100 keV than the Bremsstrahlung beam (which extends far into the MeV range). The large field of view permits us to measure the beam divergence. We observed a FWHM beam divergence of  $\Theta_x = (12.7 \pm 3.6)$  mrad and  $\Theta_y = (13.0 \pm 4.0)$  mrad, where  $x$  is plane of laser polarization. The pointing stability are 8.3 mrad and 6.4 mrad, respectively. The duration of the pulse is approximately given by the electron bunch duration [15], which is a few femtoseconds for electrons beams in our regime of operation.

To get a better estimate of the X-ray spectrum, we simulated the interaction between the electron bunch and the laser in a test particle model using PLARES [16]. For these simulations we used an electron beam of 140 MeV peak energy, 5 percent energy spread and 5 mrad divergence, similar to the electron beam distributions shown in Fig.2. Not included in this model is the dark current, which will contribute to the low energy tail of the spectrum. We modeled the scattering pulse as a counter-propagating laser pulse of  $a_0 = 1.0$  and 30 fs duration. For such beam parameters the backscattered radiation fields add up incoherently and as shown in Fig.3 we observe that the resulting radiation spectrum is much broader than the initial electron spectrum. The large energy spread is a consequence of the elevated undulator strength parameter  $a_0 = 1.0$ , the initial electron energy spread and the electron beam divergence. Simulations

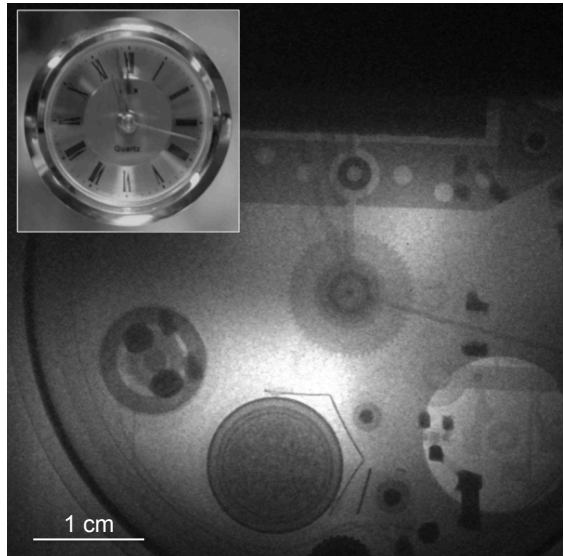


FIG. 4. Single shot radiography of a clock, with a photography as inlet. Different materials are clearly identifiable. The dark area in the upper part is a shadow cast by the dipole magnet employed to measure the electron spectrum. The signal values measured in this area are used to estimate the background signal. Signal outliers have been removed.

for various beam parameters show that the latter is usually the dominating effect for laser-accelerated electron beams. Taking into account the missing dark current contribution in the simulation and the reduced scintillator response at higher photon energies, our results are in fair agreement with the experimental data.

To demonstrate that the X-ray flux from Compton backscattering is sufficient for imaging applications, we performed radiographs of macroscopic objects, placed in front of the detector. As an example Fig.4 shows the radiograph of a clock. Its structural parts consist of different metal alloys, while the gears are made of plastic. The different material are clearly distinguishable in the radiograph due to their distinct absorption coefficients. As discussed previously the bremsstrahlung component is very energetic ( $> 100$  keV) and therefore adds to the image mostly in form of a subtractable background noise. Due to the small source size [13] a subject placed closer to the source will show significant edge enhancement (propagation-based phase contrast imaging).

In conclusion we have performed experiments on Compton-backscattering of an intense laser with electrons from a laser-plasma accelerator. The micrometer-size optical undulator period leads to the emission of radiation of hundreds of keV, well beyond energies obtained with other femtosecond sources as for example betatron sources or free-electron lasers [15]. Laser-wakefield based Compton scattering therefore provides unique properties that may be of interest for pump-probe experiments, e.g. in initial fusion research. Beyond applications in fundamental research, the source has also promising properties for medical and industrial applications. In particular we have shown that the single-shot photon flux is sufficient for imaging of macroscopic objects. Due to the inherent micrometer source size the source is suitable for phase contrast imaging techniques, which will be an area of future investigations.

**ACKNOWLEDGMENTS:** We acknowledge the Agence Nationale pour la Recherche through the FENICS Project No. ANR-12-JS04-0004-01, the Agence Nationale pour la Recherche through the FEMTOMAT Project No. ANR-13-BS04-0002, LA3NET project (GA-ITN-2011-289191), and GARC project 15-03118S.

- 
- [1] Jackson J D 1990 *Classical Electrodynamics* 2nd ed (New York: Wiley)
  - [2] Bilderback D H, Elleaume P and Weckert E 2005 *Journal of Physics B-Atomic Molecular and Optical Physics* **38** 773–797
  - [3] Faure J, Glinec Y, Pukhov A, Kiselev S, Gordienko S, Lefebvre E, Rousseau J P, Burgy F and Malka V 2004 *Nature* **431** 541–544
  - [4] Geddes C G R, Toth C, van Tilborg J, Esarey E, Schroeder C B, Bruhwiler D, Nieter C, Cary J and Leemans W P 2004 *Nature* **431** 538–541
  - [5] Mangles S P D, Murphy C D, Najmudin Z, Thomas A G R, Collier J L, Dangor A E, Dival E J, Foster P S, Gallacher J G, Hooker C J, Jaroszynski D A, Langley A J, Mori W B, Norreys P A, Tsung F S, Viskup R, Walton B R and Krushelnick K 2004 *Nature* **431** 535–538
  - [6] Esarey E, Schroeder C B and Leemans W P 2009 *Reviews of Modern Physics* **81** 1229–1285
  - [7] Leemans W P, Nagler B, Gonsalves A J, Toth C, Nakamura K, Geddes C G R, Esarey E, Schroeder C B and Hooker S M 2006 *Nature Physics* **2** 696–699
  - [8] Fritzier S, Lefebvre E, Malka V, Burgy F, Dangor A E, Krushelnick K, Mangles S P D, Najmudin Z, Rousseau J P and Walton B 2004 *Physical Review Letters* **92** 165006
  - [9] Lundh O, Lim J, Rechatin C, Ammoura L, Ben-Ismaïl A, Davoine X, Gallot G, Goddet J P, Lefebvre E, Malka V and Faure J 2011 *Nature Physics* **7** 219–222
  - [10] Lau Y Y, He F, Umstadter D P and Kowalczyk R 2003 *Physics of Plasmas* **10** 2155–2162
  - [11] Powers N D, Ghebregziabher I, Golovin G, Liu C, Chen S, Banerjee S, Zhang J and Umstadter D P 2013 *Nature Photonics* 1–4
  - [12] Khrennikov K, Wenz J, Buck A, Xu J, Heigoldt M, Veisz L and Karsch S 2015 *Physical Review Letters* **114** 195003
  - [13] Ta Phuoc K, Corde S, Thauray C, Malka V, Tafzi A, Goddet J P, Shah R C, Sebban S and Rousse A 2012 *Nature Photonics* **6** 308–311
  - [14] Tsai H E, Wang X, Shaw J, Li Z, Arefiev A V, Zhang X, Zgadzaj R, Henderson W, Khudik V, Shvets G and Downer M C 2015 *Physics of Plasmas* **22** 1–10
  - [15] Corde S, Ta Phuoc K, Lambert G, Fitour R, Malka V, Rousse A, Beck A and Lefebvre E 2013 *Reviews of Modern Physics* **85** 1–48
  - [16] Andriyash I A, Lehe R and Malka V 2015 *Journal of Computational Physics*